MICROCOPY RESOLUTION TEST CHART
NATIONAL BUREAU OF STANDARDS-1963-A

TR-2320

⛵

DAVIDSON
LABORATORY

Technical Report SIT-DL-83-9-2320
January 1983

INTEGRATED BOW WATERJET FOR
AMPHIBIOUS VEHICLES

by

Edward Numata

STEVENS INSTITUTE
OF TECHNOLOGY

CASTLE POINT STATION
HOBOKEN, NEW JERSEY 07030

DTIC
ELECT
APR 2 4 1984

A

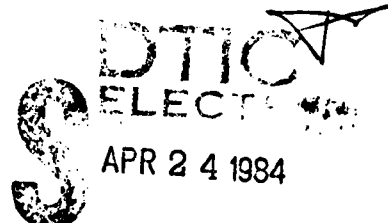TR-2320

REPORT DOCUMENTATION PAGE		READ INSTRUCTIONS BEFORE COMPLETING FORM
1. REPORT NUMBER SIT-DL-83-9-2320	2. GOVT ACCESSION NO. AD-A140 392	3. RECIPIENT'S CATALOG NUMBER
4. TITLE *(and Subtitle)* INTEGRATED BOW WATERJET FOR AMPHIBIOUS VEHICLES		5. TYPE OF REPORT & PERIOD COVERED Interim Report September 1981 – January 1983
		6. PERFORMING ORG. REPORT NUMBER
7. AUTHOR(s) Edward Numata		8. CONTRACT OR GRANT NUMBER(s) N00014-80-D-0890 Delivery Order 4, Item 2 Project NR 062 669
9. PERFORMING ORGANIZATION NAME AND ADDRESS DAVIDSON LABORATORY Stevens Institute of Technology Hoboken, N. J. 07030		10. PROGRAM ELEMENT, PROJECT, TASK AREA & WORK UNIT NUMBERS
11. CONTROLLING OFFICE NAME AND ADDRESS David W. Taylor Naval Ship Research and Development Center Bethesda, MD 20084		12. REPORT DATE January 1983
		13. NUMBER OF PAGES 22
14. MONITORING AGENCY NAME & ADDRESS*(if different from Controlling Office)* Office of Naval Research, Code 438 800 N. Quincy Arlington, VA 22217		15. SECURITY CLASS. *(of this report)* Unclassified
		15a. DECLASSIFICATION/DOWNGRADING SCHEDULE

16. DISTRIBUTION STATEMENT *(of this Report)*

   Approved for public release: distribution unlimited.

17. DISTRIBUTION STATEMENT *(of the abstract entered in Block 20, if different from Report)*

18. SUPPLEMENTARY NOTES

19. KEY WORDS *(Continue on reverse side if necessary and identify by block number)*

   Amphibious Vehicle
   Waterjet Propulsion
   Model Test

20. ABSTRACT *(Continue on reverse side if necessary and identify by block number)*
   Experiments were conducted with a scale model of an amphibious vehicle towed in calm water. Pressure distribution along the submerged bow and hull bottom was determined for a range of vehicle speed. A waterjet system with a bow intake and an axial flow impeller were then installed. The effect of the waterjet on bottom pressure distribution and height of bow wave were determined.

DD FORM 1473 1 JAN 73   EDITION OF 1 NOV 65 IS OBSOLETE
S/N 0102-014-6601 ,

STEVENS INSTITUTE OF TECHNOLOGY
DAVIDSON LABORATORY
Castle Point Station, Hoboken, New Jersey 07030

Technical Report SIT-DL-83-9-2320

January 1983

INTEGRATED BOW WATER JET

FOR AMPHIBIOUS VEHICLES

By

E. Numata

Prepared for

David W. Taylor Naval Ship R&D Center

Accession For

DTIC
COPY
INSPECTED
2

APPROVED:

Daniel Savitsky
Acting Director

INTRODUCTION

The conventional location of the water-jet propulsion system in the stern of amphibious vehicles has several hydrodynamic disadvantages which result in low efficiencies. These include:

1) The necessity for using relatively small diameter water-jet nozzles which have inherently low efficiencies.

2) The location of water intakes in an area seriously obstructed by tracks which results in significant intake losses.

To overcome these disadvantages, it seemed desirable to examine the potential of relocating the water jet into more favorable regions of the hull. For example, the water jet intake could be placed in the high pressure area under the bow with side discharge just aft of the bow. The potential hydrodynamic advantages of such an arrangement would include:

1) Location of the water-jet intake in a positive pressure area will develop some ram effect but more important, the intakes will be in a relatively unobstructed flow environment.

2) If properly integrated into the bow design, it was hoped that the intake flow could be made to interact with the bow wave, reduce its height, and thus reduce the bow wetting and hull resistance.

An experimental approach, utilizing a scale model of an amphibious vehicle, was adopted to evaluate the bow intake concept. The test program consisted of two phases:

1. Determine the pressure distribution along the submerged bow and hull bottom of the existing vehicle.

2. Modify model by installing a bow intake, internal ducting, an axial flow impeller, and discharge ports; determine effect of water-jet intake on the bottom pressure distributions, bow wave, hull trim and heave.

The model used for the present test program was one of four models built for an investigation of coupled vehicles, in support of the Marine Corps Surface Mobility Exploratory Development Plan. The following description of the model is excerpted from Reference 1:

"The models used in this investigation are representative of current operational amphibians. In consultation with NSRDC, Code 112, a simplified version of the LVTP-7 was chosen, referred to herein as the LVT design. The models were to be representative of both 14-ton and 26-ton vehicles, a 1/9-scale for the 26-ton version and a 1/7.3 scale for the 14-ton version. In its hydrodynamic configuration the LVT has side and bottom covers over its fully retracted tracks, and the track cavities are flooded. Simulated wheels and tracks were added and enclosed by side and bottom covers. The ends of the track wells were left open to allow for drainage."

The only change in the above configuration was to modify the bow to more closely represent the basic LVTP-7 bow, as shown in Figure 1.

Tests were carried out in the Tank No. 3 facility of the Davidson Laboratory. Phase 1 pressure measurements were conducted during four test sessions from mid-October to early-November 1982. Phase 2 "bow suction" tests were conducted on December 1, 1982.

PHASE I
PRESSURE SURVEY

Since both Phases 1 and 2 were primarily exploratory, the guiding principles of the experiments were to (1) make use of existing instrumentation coupled with known techniques, and (2) design the experiment so as to make efficient use of test time while obtaining sufficient information on pressures to provide:

a. Explanations of undesirable wave formations and vehicle attitudes such as sinkage and bow-down trim.

b. Guidance on a suitable location for a bow water jet intake.

Pressure Measurement Technique

Figure 2 shows the locations of 18 pressure taps on the longitudinal centerline and starboard side of the model. In-house pressure gages with ratings suitable for measuring anticipated pressure changes of several inches of water were used. To minimize the length of water-filled tubing between each gage and a pressure tap, all gages were mounted within the model.

The pressure measured at a given location develops through the following stages:

    a. Static head h_o with model at rest.

    b. Static head change δh due to sinkage and trim changes
       of moving model relative to at-rest attitude.

    c. Dynamic head, h .

Measured static pressure h_o was used as the basic datum. Measured pressure h_m on the moving model was $h_m = h_o + \delta h + h$. Since a dynamic pressure distribution was desired, it was necessary to measure sinkage and trim changes relative to the at-rest datum, and then calculate the associated change in head δh. Then dynamic head $h = h_m - h_o - \delta h$.

Appendix A gives details of test instruments and pressure data processing procedures, page 10.

Test Program

Review of earlier tests of LVTP-7 models in calm water, Reference 2, showed that the two loading conditions investigated experienced generally similar behavior. As speed increased, sinkage and bow-down trim increased until vehicle operations were hampered by excessive water over the bow. Thus, for the present exploratory tests, either condition could be used in the interests of minimizing test time. The "Combat Equipped" loading, i.e., without troops in the personnel compartment aft, was chosen since previous tests[2] showed that because of an initial bow down trim of about 2½ deg, the vehicle had an operational speed limit of 8 mph due to excessive water over the bow at that speed. Speeds of 4, 5, 6 and 7 mph were chosen for the present tests.

Test Results

Measured pressures were processed to remove the static head component, and the resulting dynamic heads h were compared to stagnation pressure expressed as $h_s = 12V^2/2g$ inches of water. Figure 3 shows the distribution of h/h_s along the centerline of the vehicle; Figure 4 shows the distribution of h/h_s at 0.43 (hull beam). Also superimposed on the two figures is an approximation of the wave profiles on the side of the vehicle at speeds of 4 and 7 mph, as taken from photographs. The similarity between pressure distributions and wave profiles is obvious.

The abrupt transition between the bow rake and the flat bottom of the vehicle hull causes an acceleration of flow and a sharp drop in pressure. As vehicle speed increases, the negative pressures intensify to increase sinkage and bow-down trim because the dynamic head ordinates of Figures 3 and 4 are proportional to the square of speed.

PHASE 2
BOW SUCTION TESTS

Ideally, a bow jet propulsion system would have bottom-mounted bow intakes port and starboard near the sides of the hull, and discharge ports a short distance aft of the bow, with an impeller between intake and discharge. However, designing, constructing and retrofitting such a system in the existing amphibian model would have been difficult and costly. An alternative system was devised using a single central impeller drawing water through a single bow intake and discharging through port and starboard ducts. This latter system was fitted in the model without requiring extensive modification of existing structure. Figure 5 shows photographs of the installation which was assembled using an electric drive motor with a feedback speed control, and an impeller capable of absorbing motor torque over a wide range of shaft speeds.

The objective of this phase of testing was to determine the effect on vehicle sinkage, trim, and pressure distribution due to sucking water through the bow intake. Design of the experiment, model details, test procedure, and test results are described in the sections which follow.

Experiment Design

In evaluating the effect of bow suction on the behavior of the vehicle, it was important to take account of the water flowing through intake, ducting and discharges. Plan and side elevation views of the model ducting system, Figure 6, indicate a significant weight of water fills the ducting when the impeller is working. Thus, to assure an equivalence of test conditions, the experiment was planned as follows:

1. A control condition for vehicle behavior was established by towing the modified model with ducting blocked to prevent flow.

2. In anticipation that pumped flow through the duct system might cause a change of trim, the model was towed at fixed trims in both the control test and in the pumped flow test. If pumping should alter the pressure distribution, such a change would be monitored by measuring (a) pressures at two critical locations and (b) model trimming moment in both tests.

3. Although fixed in trim, the model was towed free to heave. Heave was monitored and any increase in sinkage, due to the added weight of water when pumping, was compensated by unloading the heave mast.

4. Flow rate was varied by changing

   a. Impeller motor speed
   b. Bow intake area

The Phase 1 tests showed that over the speed range of 4 to 7 mph, trends in pressures and vehicle attitude were gradual and predictable. Because of the greater variety of parameter changes in Phase 2, vehicle speeds were limited to 4 and 7 mph to keep the test matrix at a manageable level.

Model Details

As noted on page 4 , the ducting and impeller assembly were designed for simplicity of fabrication and ease of installation in an existing model.

The photographs in Figure 5 show that the drive motor and all ducting were installed on the inner bottom of the model. The intake nozzle was designed to span the full width of the bow, below the bow knuckle and above the inner bottom. Figures 5 and 6 show the transition from oval-shaped intake to a circular duct housing the impeller. Figure 5 also shows the location of a discharge opening just above the track well on the starboard side.

The intake nozzle opening illustrated in Figure 5 has an area 1.4 times the area of the 3-inch i.d. central duct; an alternate nozzle area was 1.1 times the duct area.

The impeller, shown in Figures 5 and 6, was a stock 4-bladed marine propeller model having the following principal characteristics

Diameter (= Pitch)	2.90 in
Hub diameter	0.56 in
Developed Area Ratio	0.83

The central location of the intake nozzle, ducting, and motor drive unit precluded the use of any of the centerline pressure taps employed in Phase 1. Two taps on the starboard side, located in the negative pressure region, were used to monitor pressure changes. Appendix A contains details of instrumentation and measurement techniques, pages 11 and 12.

Test Results

Measured pressure was processed to remove the static head component, and the resulting dynamic head h was compared to stagnation pressure $0.5\rho V^2$ expressed as h_s inches of water. Figure 7 presents plots of h/h_s as a function of fixed trim angle at 4 mph and 7 mph. The plots show that pumped flow through the bow intake causes only a small change in dynamic head at pressure tap "C" where peak negative pressure occurs. Changing the intake area ratio from 1.4 to 1.1 had little effect on peak negative pressures.

A comparison of visual observations of the model running with ducts blocked versus with pumped flow showed little change in both rise of water at the bow and in wave profile along the side of the hull. This observation

is consistent with the relatively small changes in measured pressures between the two conditions.

The objective of measuring trim moment was to monitor the integrated effect of any changes in hull pressure distribution caused by pumped flow through the duct system. It was hoped that such moment measurements would supplement the pressure data which were limited to only two locations.

In the Appendix on page 12 there is a description of the components which contributed to the total measured by the trim moment balance, including the moment due to impeller thrust.

Thrust of the impeller was estimated as described on page 13 of the Appendix. Measured model velocity and impeller rotational speed were used with published performance characteristics of a similar propeller in a cylindrical duct (References 3 and 4) to estimate impeller thrust and flow velocity through the impeller duct.

At 4 mph, there was an increase in bow down moment of 1.3 in-lb between the "duct blocked" and the "pumped flow" conditions. This net moment was caused by the following changes in component moments, where (+) is bow up and (-) bow down:

	in-lb
Additional water in duct system	-10.8
Impeller thrust	+ 4.3
Other components	+ 5.2
Net Change	- 1.3

"Other components" would include moment change due to a change in pressure distribution. The bow-up sense of this moment change is consistent with the decrease in negative dynamic head, Figure 7, caused by impeller operation. Using the measured unit trim moment, 15.6 in-lb/deg, he +5.° in-lb bow-up moment would result in a trim change of +0.3 deg for a f ee-to-trim model.

The impeller caused a substantial increase in flow compared to free-flow velocity through the duct system. Velocity increases of 65 percent at 4 mph and 55 percent at 7 mph were estimated by the calculation procedure shown on page 13. However, as noted on page 6, these significant increases in flow rate through the duct system resulted in no visible decrease in bow wave height and only a small, favorable change in dynamic pressure under the hull.

CONCLUDING REMARKS

A series of exploratory tests with a scale model of a representative amphibious, tracked vehicle has produced the following results:

- Dynamic pressure distribution along the submerged bow and bottom of a moving vehicle model was measured. The pressure distribution was consistent with the observed shape of the wave profile on the side of the vehicle.

- A sharp negative dynamic pressure peak occurred at the abrupt transition between the 40 degree bow rake slope and the flat bottom of the hull, due to acceleration of flow over the transition. This negative pressure peak, which increased as the square of vehicle speed, contributed to an increase in bow-down trim as vehicle speed increased.

- A duct system housing an impeller which accelerated water through a bow intake and discharged through ports on each side of the model, resulted in a small reduction in negative pressure at the base of the bow rake, but had no visible effect on the height of the bow wave.

- Based on these exploratory results, a water jet propulsor with bow intake appears to offer only marginal improvement in vehicle trim and no visible reduction in height of the bow wave.

- The forward location of the waterjet intakes should however have smaller intake losses and, consequently, should result in higher propulsive coefficients when compared with the usual aft location of waterjet propulsors.

REFERENCES

1. G. Fridsma and W. E. Klosinski, "A Model Study of Coupled Amphibious Vehicle Trains in Calm Water," Davidson Laboratory Report 2239, March 1982.

2. G. Fridsma and W. E. Klosinski, "Calm and Rough Water Tests of the LVT7 Series of Amphibious Tracked Vehicles," Davidson Laboratory Report 2276, October 1982.

3. J. D. van Manen, "Open-Water Test Series with Propellers in Nozzles," International Shipbuilding Progress, Volume 1, No. 2, 1954, pg. 99.

4. W.P.A. van Lammeren, J. D. van Manen and M.W.C. Oosterveld, "The Wageningen B-Screw Series," Trans. SNAME 1969, pg. 273.

APPENDIX A

Phase 1 Pressure Instrumentation and Test Procedure

Figure 2 shows the locations of 18 pressure taps on the centerline and starboard side of the model. Each tap consisted of a 0.25 inch o.d. by 0.18 inch i.d. aluminum tube with its axis normal to the outer bottom of the model; the tube end was flush with the model bottom. The upper end of each tube was connected to a pressure gage by a short length of flexible, transparent plastic tubing; the aluminum tube and plastic tubing were filled with water, free of entrapped air bubbles.

Five pressure gages, rated at 0 to 10 inches of water with respect to an atmospheric datum, were mounted in the bow of the model. Water pressure acts on the interior of a diaphragm capsule in the gage housing while the air space surrounding the capsule is vented to the atmosphere. Water pressure change causes the capsule to expand and the expansion is sensed by a linear motion transducer which results in a change in voltage output.

Pressure gages were calibrated at the start of each test day. The gages were connected through a manifold to a pressurized air accumulator with throttle valve; the throttled pressure was measured by a precision mechanical gage with a resolution of 0.05 inches of water. A five-point calibration of the electrical output of each gage furnished a linear rate obtained by a least squares technique.

Trim relative to the model baseline was sensed by an inclinometer mounted in the model. The model was towed through a pitch pivot located at the model CG, 16.9 inches aft of the bow. Change in sinkage at the CG was sensed by the vertical motion of the heave mast attached to the pitch pivot.

The signals from pressure and motions transducers were carried by overhead cable from the towing carriage to tankside signal processors and thence to an analog chart recorder. Signals were also digitized and averaged by the tankside PDP-8e digital computer.

10

Phase 2 Instrumentation and Procedure

Pressures, trim and heave were measured as in the Phase 1 tests.

Impeller motor shaft speed was determined by means of a digital frequency meter which counted the electrical pulses generated by a ten-tooth wheel on the shaft. The output of a tachometer-generator, driven by the motor shaft, was used in a feedback circuit to maintain a preset motor speed.

Prior to a test run, while the towing carriage was at rest, the impeller motor was brought up to speed using a control mounted on the carriage. When the model was advancing at steady speed, satisfactory pump flow was obtained only at certain impeller motor speeds. By trial, it was found that impeller speed n, intake area ratio $\overline{AR}$ and towing velocity V could be correlated through the ratio $(\overline{AR})V/n$ (similar to advance ratio $J = V/nd$).

Vehicle mph	Model V,ft/sec	Intake $\overline{AR}$	Impeller n, rps	$(\overline{AR})V/n$
4	1.96	1.4	21	.13
7	3.42	1.4	34	.14
7	3.42	1.1	29	.13

Pump flow would fall sharply if impeller speed increased or decreased by more than 3 rps from the above values.

The model was fixed in trim, and trim moment was sensed by a standard moment balance. A "rocker plate", placed between the balance and the model deck, was used to vary the fixed trim attitude of the model. The balance was calibrated by applying a range of known moments; the electrical output of the moment transducer furnished data for obtaining a linear rate by a least squares technique.

The placement of moment balance and rocker plate on the model is illustrated in Figure 6. Since the reference axis for moment coincided with the pivot axis of the rocker plate, and was above the model CG, an increase in bow down trim resulted in an aftward shift of the CG relative

to the moment axis. Such a shift caused the moment balance to register
a bow up weight moment; the bow down trim increase also resulted in a
bow up hydrostatic moment with the model at rest. This combined static
moment at a given fixed trim angle was used as the moment datum from which
moment changes on the moving model were measured.

When the model was advancing at fixed trim with the ducting system
blocked, the moment balance registered a bow down dynamic moment due to

    a. Drag force on the hull.

    b. Summation of moments of vertical components of dynamic pressure.

With the model advancing at fixed trim and the impeller working, a
further change in moment was caused by:

    a. A bow down increment due to a change from blocked ducts
       partly filled with water to completely filled ducts when
       pumping (the center of duct volume is forward of the
       moment axis).

    b. A bow down increment due to viscous drag of water flowing
       through the duct system.

    c. An increment caused by flow changes along the hull due to
       alterations in pressure distribution.

    d. A bow up increment due to impeller thrust.

Estimate of Impeller Performance

Accelerated flow through the discharge ports was clearly visible
when the model was moving. The following analysis uses published data on
performance of a marine propeller in a cylindrical duct to estimate (a) the
thrust delivered by the impeller, and (b) flow velocity in the impeller duct.

Reference 3 gives characteristic curves of a four-bladed marine pro-
peller in an axial circular cylinder; Reference 4 presents curves for the
same propeller in open water. Curves of thrust coefficient K_T versus advance
coefficient J, excerpted from References 3 and 4, are given in Figure 8
(Wageningen B series propeller, 4 blades, expanded area ratio = 0.55 and pitch

ratio P/d = 1.0). Also shown on Figure 8 is the open water K_T versus J curve for the DL propeller used in the present tests (4 blades, area ratio = .83, P/d = 1.0). It is evident that the open water characteristics of the B Series and DL propellers are similar. Thus, we will assume that the B Series curve of K_T vs J in an axial circular cylinder can be used for an approximate analysis of the performance of the DL propeller in the present duct system. Reference 3 also reports a comparison between the advance velocity V of the "screw plus axial cylinder" and mean velocity in the cylinder V_c measured by pitot tube; this comparison is reproduced on Figure 8 as a curve of $J_c = V_c/nd$ versus the usual advance ratio J.

The thrust T associated with a water jet is the time rate of change of momentum of the jet fluid. Thus, $T = \rho Q(\delta V)$ where Q is volume flow rate and δV is the velocity increment imparted by the impeller. By continuity of flow $Q = V_c A_c$ where A_c is the cross-sectional area of the impeller duct. Since there is an increase in entrance velocity due to the ratio $\overline{AR}$ of intake area to impeller duct area, $V_c = \overline{AR}V + \delta V$.
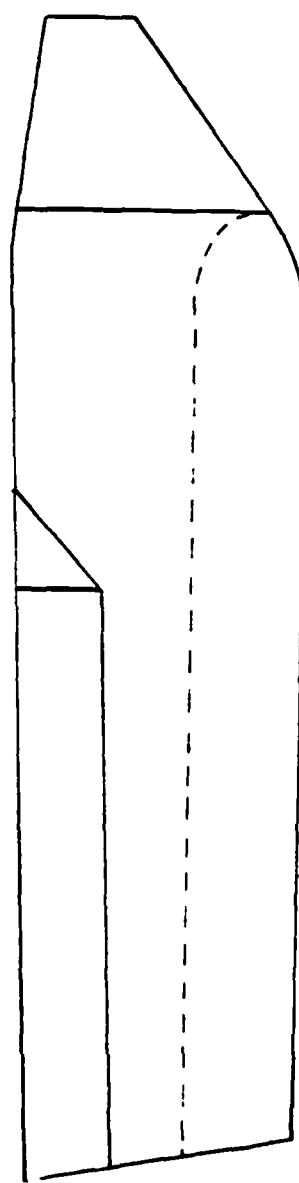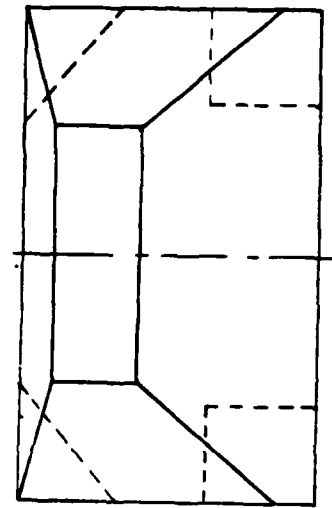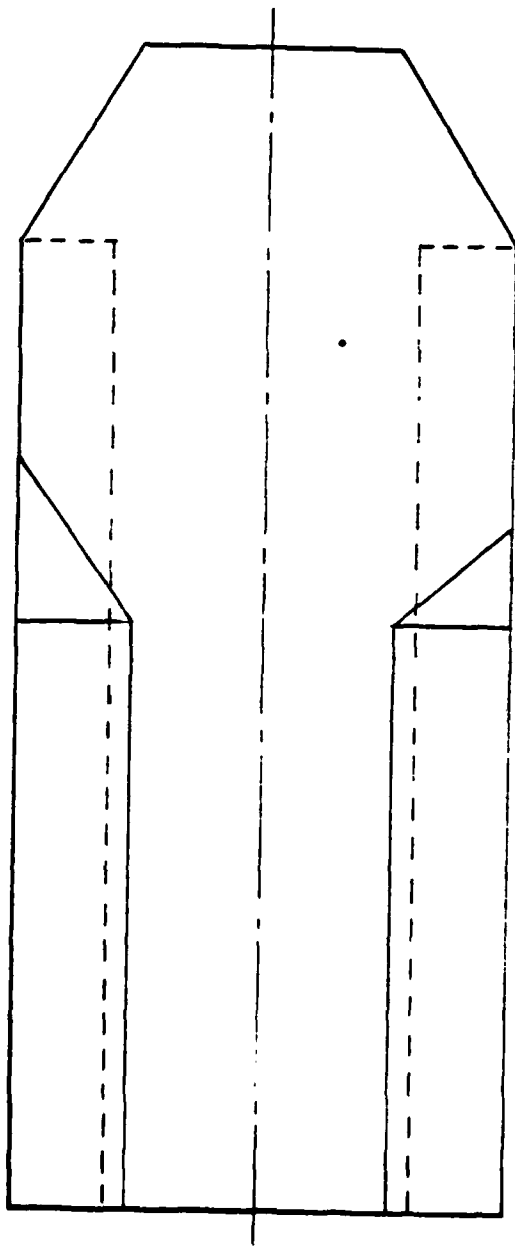
Substituting,

$$T = \rho A_c (\overline{AR}V + \delta V) \delta V \qquad [1]$$

For a given model speed V and measured impeller speed n, the following calculation procedure was used to estimate the operating point of the impeller.

   a. Assume values of δV and calculate T.

   b. Calculate $K_T' = T/\rho n^2 d^4$ where d is impeller duct diameter.

   c. From $V_c = \overline{AR}V + \delta V$, calculate $J_c = V_c/nd$.

   d. On Figure 8, enter J_c on curve of J_c vs J and read J.

   e. Plot K_T' vs J and where it intersects curve of K_T vs J for propeller in cylinder is operating point.

   f. At operating point read K_T and J_c; calculate $T = K_T \rho n^2 d^4$, and $V_c = J_c nd$.

13

Results were as follows for the basic area ratio $\overline{AR} = 1.4$:

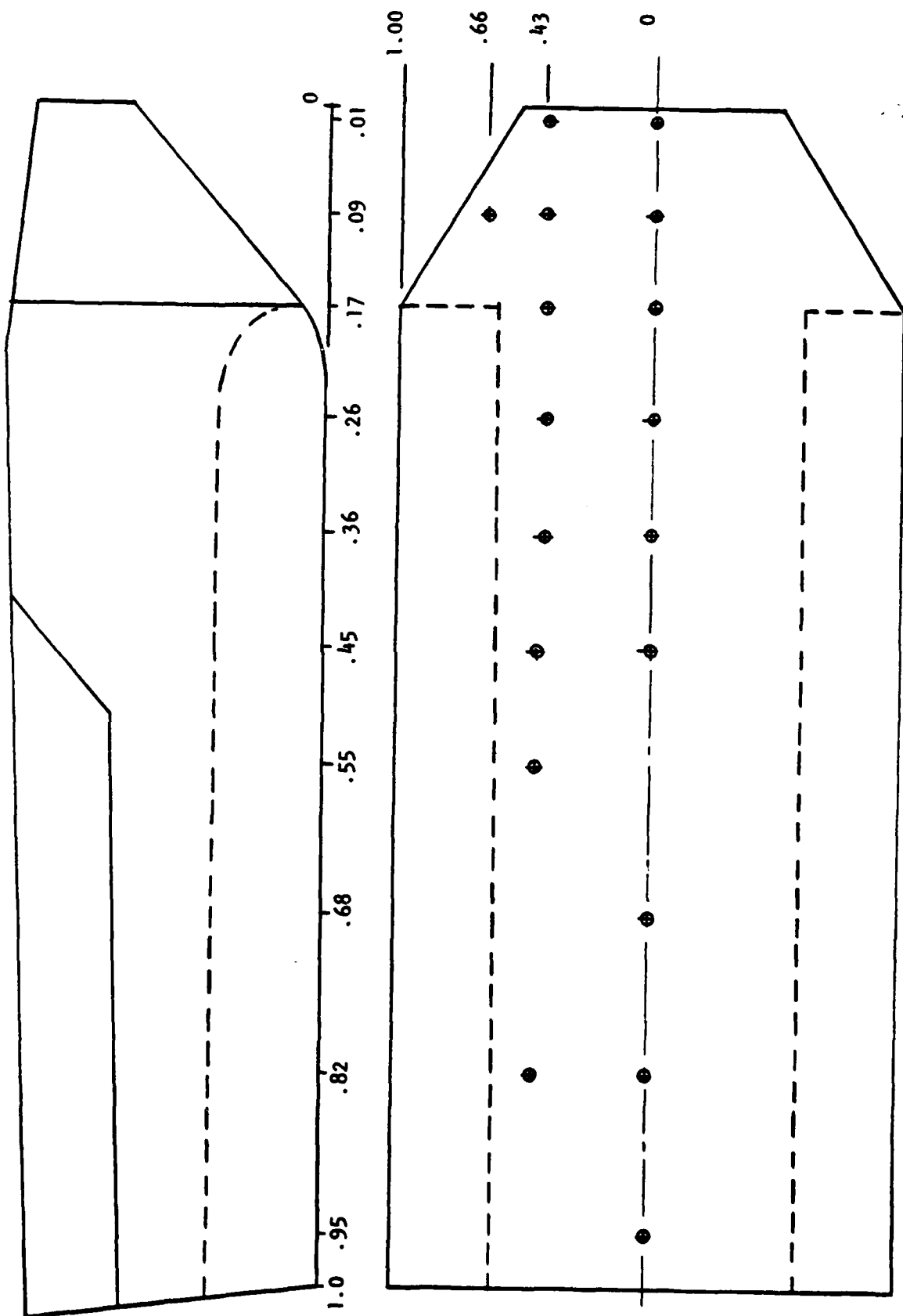| mph	V,ft/sec	Calculated	
		T,lb	V_c,ft/sec
4	1.96	0.8	4.55
7	3.42	1.9	7.45

Track Well

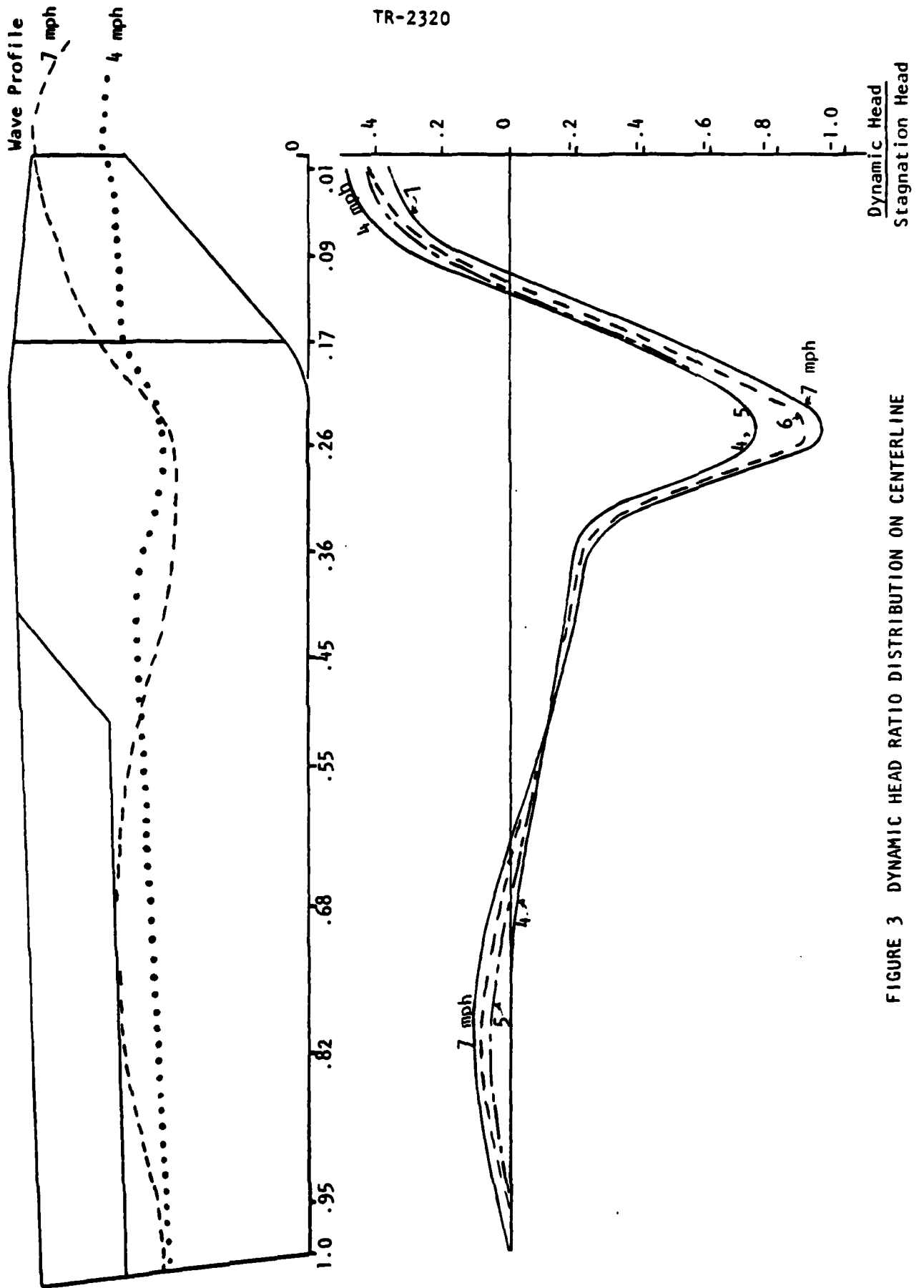FIGURE 1 MODEL CONFIGURATION

FIGURE 2 LOCATIONS OF PRESSURE TAPS
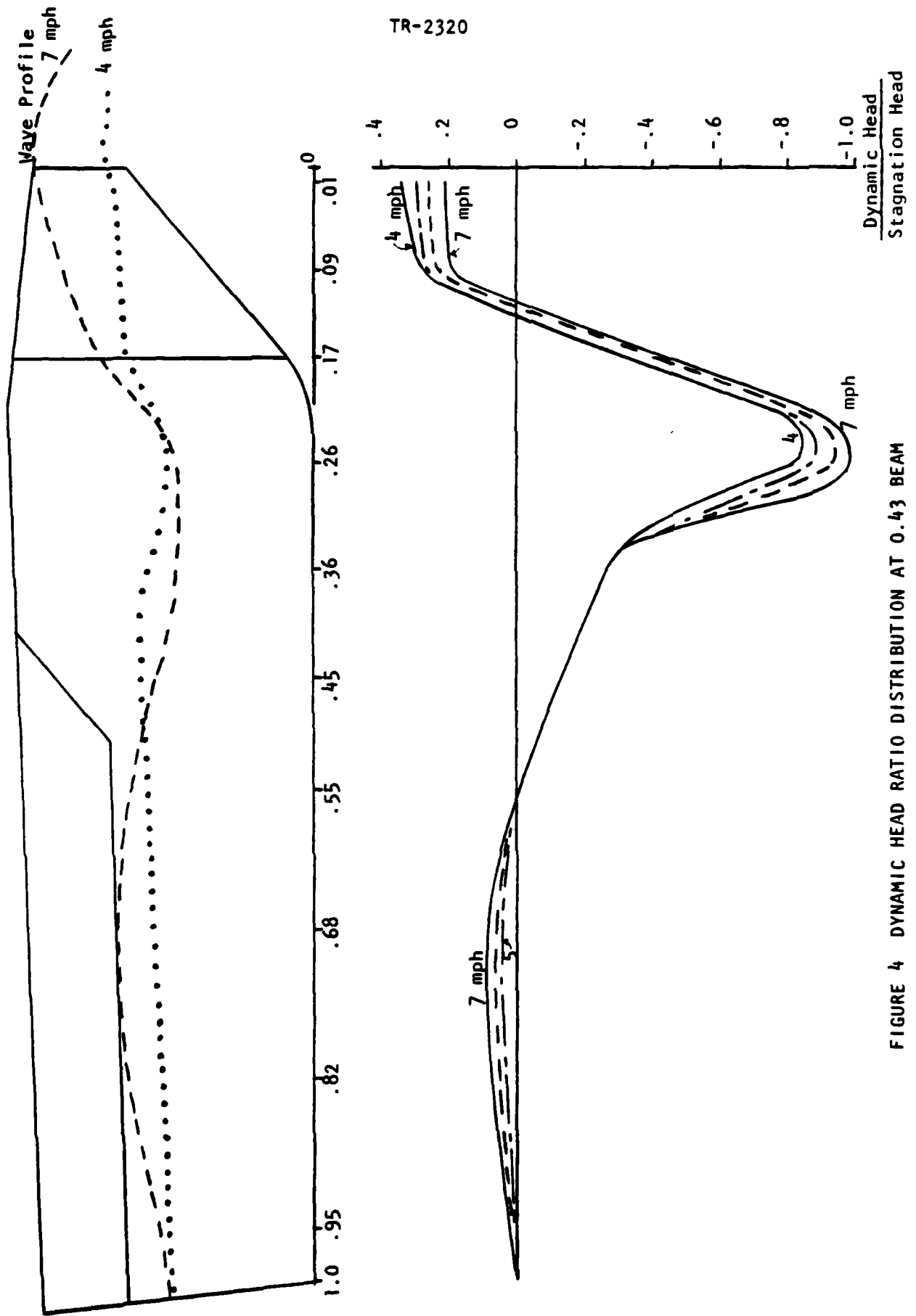
FIGURE 3   DYNAMIC HEAD RATIO DISTRIBUTION ON CENTERLINE

FIGURE 4 DYNAMIC HEAD RATIO DISTRIBUTION AT 0.43 BEAM
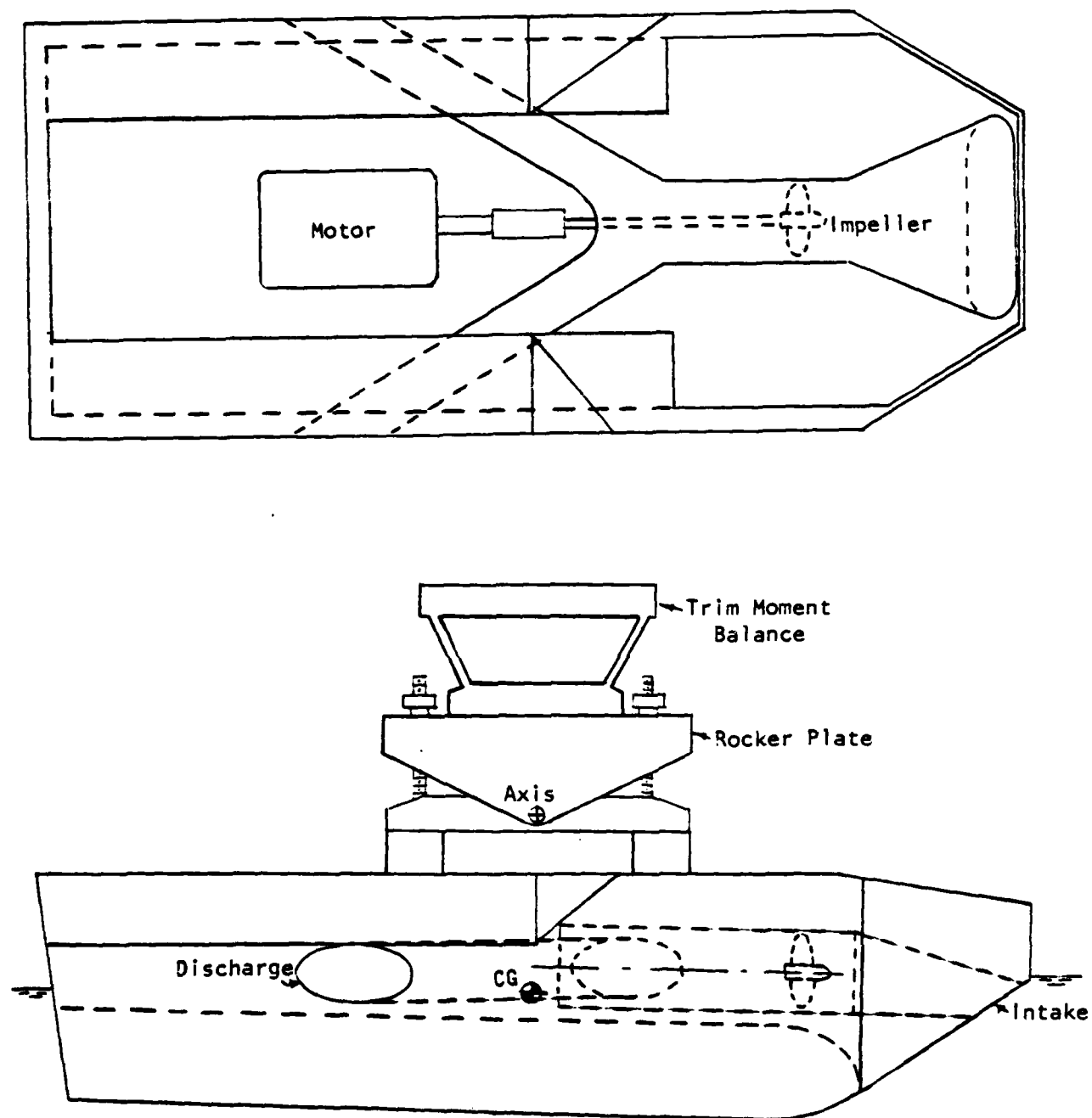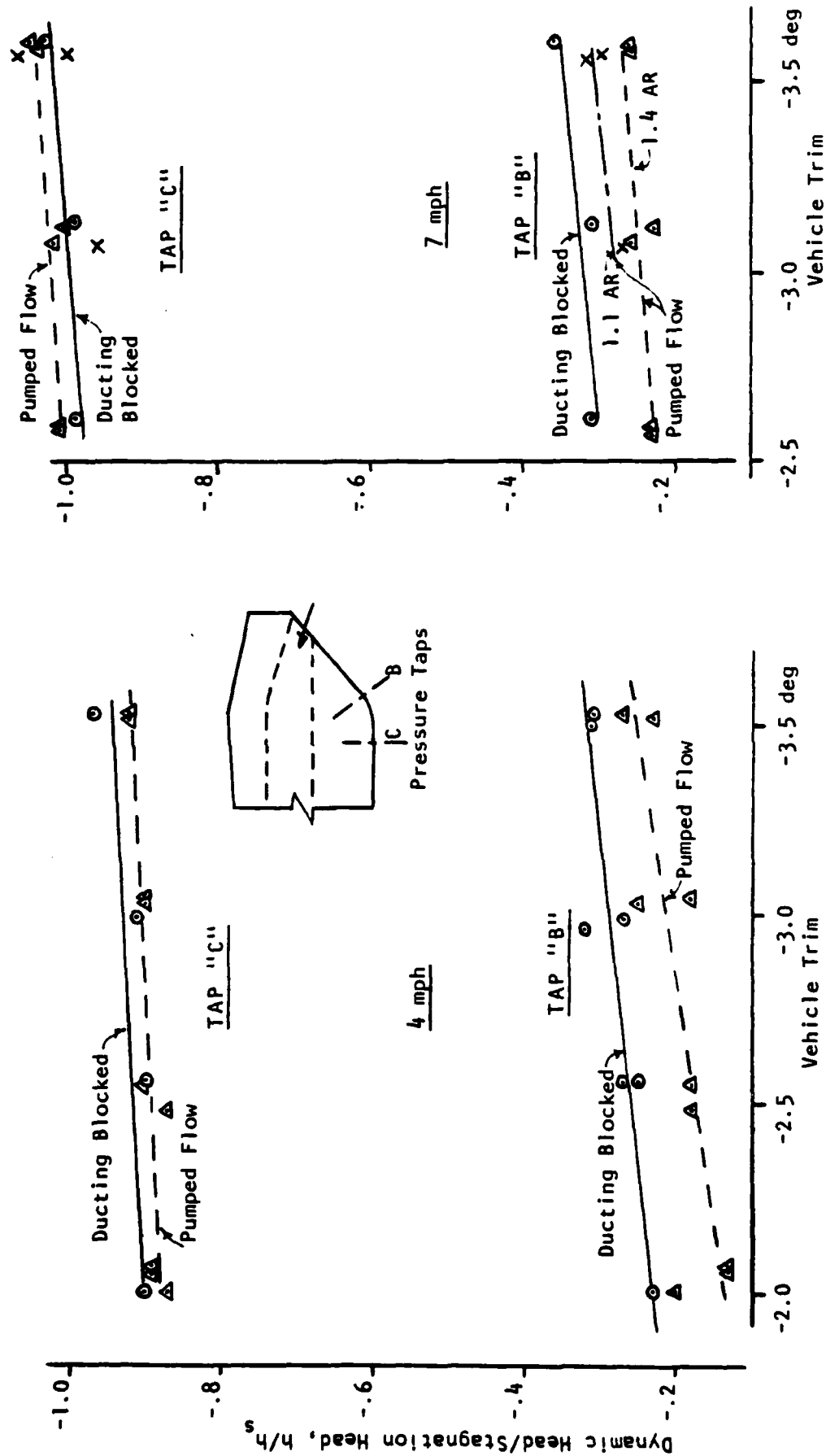
FIGURE 5

FIGURE 6 DUCTED MODEL
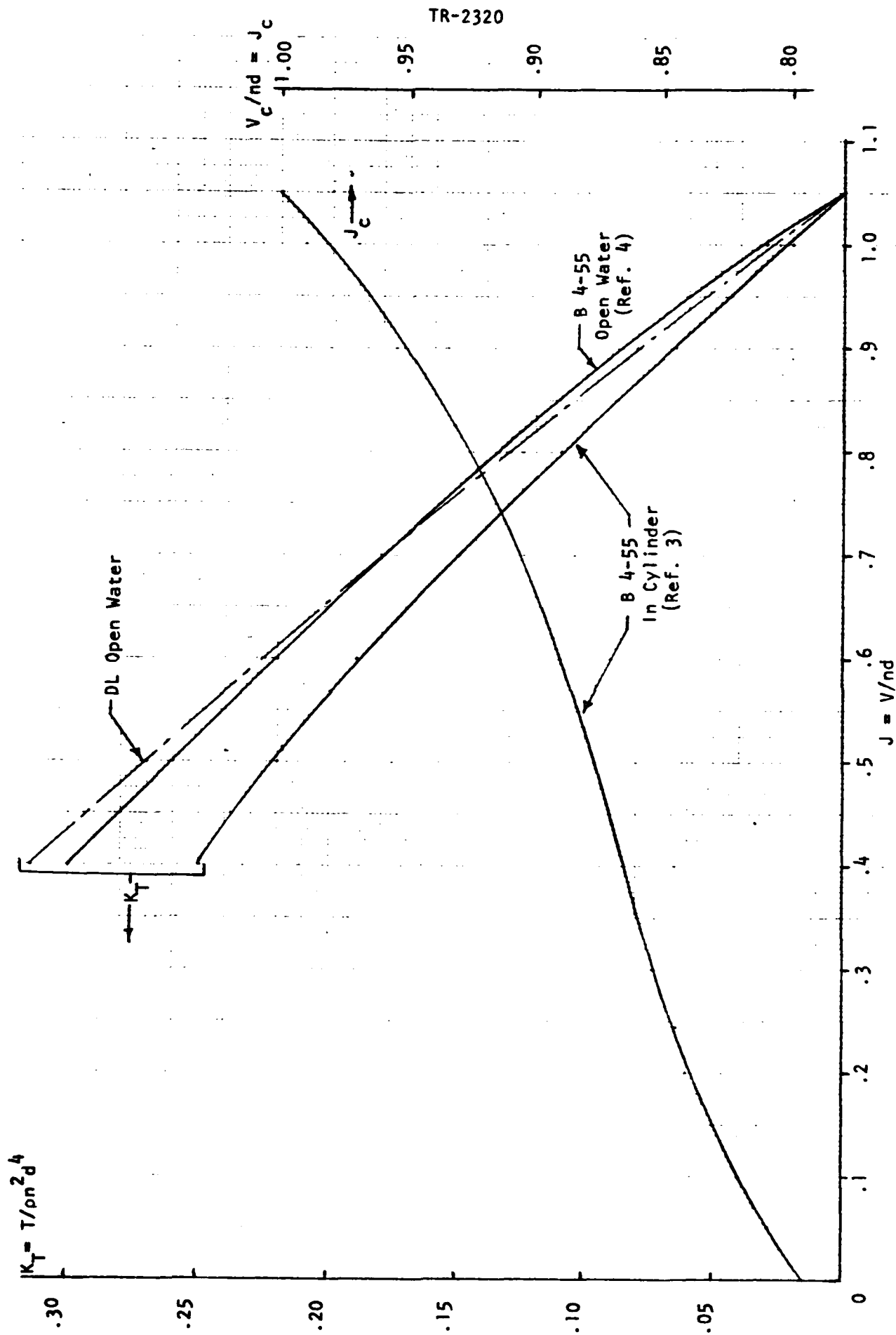
FIGURE 7   EFFECT OF BOW SUCTION ON DYNAMIC HEAD RATIO

FIGURE 8 PROPELLER CHARACTERISTIC CURVES

DISTRIBUTION LIST
(Contract N00014-80-D-0890)

Copies	
6	DAVID W. TAYLOR NAVAL SHIP RESEARCH AND DEVELOPMENT CENTER Bethesda, MD 20084 Attn: Code 1120
1	OFFICE OF NAVAL RESEARCH 800 N. Quincy Street Arlington, VA 22217 Attn: Code 438
1	OFFICE OF NAVAL RESEARCH Branch Office Building 114, Section D 666 Summer Street Boston, MA 02210
1	OFFICE OF NAVAL RESEARCH Resident Representative 715 Broadway, 5th Floor New York, NY 10003
12	DEFENSE TECHNICAL INFORMATION CENTER Building 5, Cameron Station Alexandria, VA 22314

END

FILMED

6-84

DTIC